# Interactive Acquisition, Analysis, and Visualization of Sonographic Volume Data

**Thomas R. Nelson, Dolores H. Pretorius**

Divisions of Physics and Ultrasound 0610, Department of Radiology, University of California, San Diego La Jolla, CA 92093-0610

*Received 6 May 1996; revised 3 September 1996*

**ABSTRACT:** This article discusses the design features of an interactive system for acquiring, analyzing, and displaying volume sonographic patient data. Methods for reprojection of two-dimensional (2D) sonographic image data into a volume matrix are discussed. We describe an intuitive, easy-to-use graphical user interface that facilitates physician operation of a system incorporating an interactive volume renderer for optimization of viewing orientation and data presentation and incorporates stereoscopic viewing. Visualization methods are described that permit the operator interactively to extract tissues or organs of interest from the rest of the volume scanned. Selected examples of clinical images are given to demonstrate system capability. The system represents a cost-effective 3D ultrasound system integrating clinical scanners and graphics workstations. © 1997 John Wiley & Sons, Inc. Int J Imaging Syst Technol, **8,** 26–37, 1997

## I. INTRODUCTION

The inherent flexibility and cost advantages of ultrasound imaging will ultimately play a large role in increasing patient throughput and reducing health care costs. Two-dimensional (2D) sonography is in routine use in nearly all American hospitals and many physician offices and clinics because it offers many benefits compared to other medical imaging techniques. Sonography offers unique qualities including real-time imaging, physiologic measurement, use of nonionizing radiation, and no known bioeffects in the diagnostic range, while being noninvasive. Sonographic imaging equipment also is far less expensive to buy and maintain than magnetic resonance imaging (MRI) and computed tomographic (CT) imaging systems. Sonographic image quality has benefitted from increasingly sophisticated computer technology. Advanced technology is now enabling 3D imaging methods to be applied to diagnostic sonography visualization with interactive manipulation of volume data using rendering, rotation, and zooming in on localized features.

Volume sonographic imaging has sparked interest in both the academic community and commercial industry, and because of the freedom to move ultrasound transducers in any plane efforts have been made to develop volume ultrasound imaging techniques combining scanning flexibility and rapid data acquisition [1–14]. Much of this effort has been directed toward integrating transducer position information with the gray-scale image to create a volume data set [15–17]. In addition, since the ultrasound signal and signal-to-noise properties are different from CT and MRI, standard volume data analysis and display techniques used in CT and MRI cannot simply be applied to ultrasound. While there has been some commercial development of volume ultrasound systems, their performance has been limited with regard to data visualization.

Current commercially available 3D ultrasound systems use several different approaches. The Combison 530 (Kretztechnik, Austria) has produced a volume sonographic machine that creates images using specially designed annular array volume transducer, hardware, and display systems. Successive images are obtained by mechanically changing the plane of the scan to sweep out a volume of data. Ultrasound data for volume visualization are obtained in $<10$ s. Among the first commercial units available, these systems are undergoing Federal Food and Drug Administration clinical trials in the United States, are being sold commercially elsewhere in the world, and have had an important impact on the clinical acceptance of volume sonography. TomTec (Boulder, CO) acquires volume data using a computer-controlled transducer carriage device executing an automated parallel plane, rotating plane, or fan plane shift in transducer orientation. Data acquisition requires several seconds to minutes with application software to analyze and display 3D reconstructions.

These systems use mechanical methods to acquire multiple slices of scan data in a constrained geometry which often limits the field of view and flexibility to optimize the patient scan. The approach presented in this article uses freehand scanning with position sensors attached to the transducer. Data from the position sensor is used to register images to each other without the constraint of scanning in a rigid geometry.

A research program in volume sonography has been under way at the University of California, San Diego (UCSD) for the past 7 years with clinical imaging trials under way in several areas ranging from the obstetric patient to carotid vascular studies. Systems integration has reached the point where routine clini-

*Correspondence to:* T. R. Nelson
*Contract grant sponsor:* ACUSON Corporation


CCC 0899–9457/97/010026-12

cal scanning is straightforward and rapid. An intuitive graphical user interface (GUI) facilitates computer interaction to reproject, filter, analyze, and display volume sonographic data on the computer screen. While additional work remains to fully realize the clinical potential of 3D ultrasound, early results clearly demonstrate the feasibility of the approach. This article discusses the methodology used to calibrate, acquire, reproject, analyze, and visualize sonographic volume data in a cost-effective system integrating clinical scanners and graphics workstations.

## II. METHODOLOGY

The volume sonography program at UCSD uses commercially available 1D transducer arrays whose position is accurately monitored by an electromagnetic position sensor, with video image capture. An intuitive GUI permits a wide range of user skill levels to operate the system and interact with volume data. Postprocessing software enhances image analysis and anatomy visualization. Preliminary work has suggested enhanced clinical utility for 3D ultrasound, and groups involved with volume sonography research have explored applications in most major organ systems including the prostate [13,18,19], carotid, cerebral and other vascular structures [12,14,20], abdomen [5,13], breast [21,22], heart [2–4,9,23,24], and fetus [1,5,7,8,25–29]. We have found that the range and depth of clinical questions asked increase as physicians have more sophisticated capability to interact with patient data. Several steps are required to calibrate, acquire, reproject, analyze, and visualize sonographic data as described in the following sections.

### A. Ultrasound Data Acquisition

*1. Hardware Configuration.* The imaging system we describe is based on using conventional ultrasound scanning systems available from a number of vendors. A block diagram of the key components is shown in Figure 1. We currently use an Acuson 128/XP-10 (Acuson Corp., Mountain View, CA) equipped with transducers ranging from 2 to 7 MHz. Gray-scale and color Doppler video image data are acquired into a graphics workstation (SPARC-10; Sun Microsystems, Mountain View, CA) equipped with a real-time 24-bit video digitizer (XVideo; Parallax Graphics, Santa Clara, CA) and stored to a high-speed digital video storage disk at 10–30 frames/s. We elected to use video image data to simplify the problem of accessing scanner image data. However, video image data limit our ability to obtain scaling and offset information available inside the scanner. As a result, it is necessary to determine image scaling calibration factors independently to reproject image planes into a volume data set and obtain quantitative data.

*2. Position Sensing.* To develop a volume data set, the position of each video frame referenced to the patient position must be known. A variety of systems have been used to obtain position tracking information, including articulated arm [30], spark-gap microphone [15], laser and infrared sensors, and electromagnetic positioning systems [11,31–33]. We currently use a 6-degree-of-freedom ($x$, $y$, $z$, $\theta_1$, $\theta_2$, $\theta_3$) electromagnetic position sensor (Fastrack; Polhemus Inc., Colchester, VT) attached to the transducer to provide position and orientation information for each image acquired (Fig. 2). This system uses a fixed point referencing the patient coordinate system and a small ($<1.0$-cm$^3$) sensor located on the transducer. The reference point source consists of a set of othogonally polarized coils that transmit a time-coded waveform through each of three coils in sequence which are detected by a sensor that also contains three orthogonally positioned coils (Operators manual; Polhemus). Our approach assumes that the only motion occurring during the scan is due to the transducer being moved across the patient. Exceptions to this may include cardiac imaging as is discussed below. Our approach preserves the flexibility of freehand scanning and does not require a predefined mechanical scanning geometry.

The position-sensing system performance necessary to obtain accurate volume reprojections is determined by scanner performance and volume scanning resolution desired (Table I). For example, to produce a voxel resolution of 0.5 mm in a 200-mm field of view (FOV) sector transducer field at the most distant location, the position sensor must have an angular resolution of at least 0.1° and a positional resolution of at least 0.25 mm. This level of performance exceeds the capability of currently available positioning systems in the clinical setting. The positioning system we employ has an angular resolution of approximately 0.5° and a position resolution of approximately 0.5 mm, which translates into a pixel resolution of 0.88 mm at 100 mm and 1.75 mm at 200 mm FOV. As scanning systems continue to improve, further improvements in position sensing approaches will need to be made to preserve system resolution.

Each type of positioning system is sensitive to its operating environment. Acoustic and light-based systems require a clear line of sight, while electromagnetic systems require a freedom from magnetic or metallic objects that can distort the field uniformity required for accurate position mapping. The system we use also is sensitive to propriety materials used in transducer construction. We currently use an offset of approximately 12 cm between the position sensor and the transducer (Fig. 2) to reduce distortion and interference between transducer materials and the position-sensing system. Calibration is necessary to correct for the offset between the position sensor and the image scan plane.

*3. Offset and Scaling Calibration.* Before clinical scanning can begin, it is necessary to determine the image-scaling calibration factors relating the video image pixel location to a physical dimension. Both the image centimeters-per-pixel scaling factor and the offset of the pixel from the transducer face and position sensor must be known to compute accurate registration values. As a result, we compute all correction factors necessary to convert each image pixel location into a coordinate in the patient reference system. The pixel intensity then is located in the volume corresponding to the physical coordinate as described below. The calibration procedure is straightforward and rapid, although each transducer and each FOV must be calibrated and involves scanning a test object we have developed. The test object consists of a small spherical latex balloon approximately 1 cm in diameter located at a depth that ranges between 20 and 100 mm to accomodate the various image FOV sizes.

Our procedure uses a two-step approach. First, we determine the image centimeters-to-pixel scaling factor by using image centimeter-depth markers and identifying the distance between two points on the computer display (Fig. 3). Second, we scan a test object from a minimum of 15 different positions to image the balloon completely from all orientations. An interactive circular cursor is positioned over the balloon image and the size adjusted to identically match the balloon. The position of the balloon center [$B(x_i, y_i)$] in the image is computed and the sensor rotation [$S(\theta_{1i}, \theta_{2i}, \theta_{3i})$] and position [$S(X_i, Y_i, Z_i)$] values for each image recorded. Next, the position of the balloon center [$B(X_i, Y_i, Z_i)$]

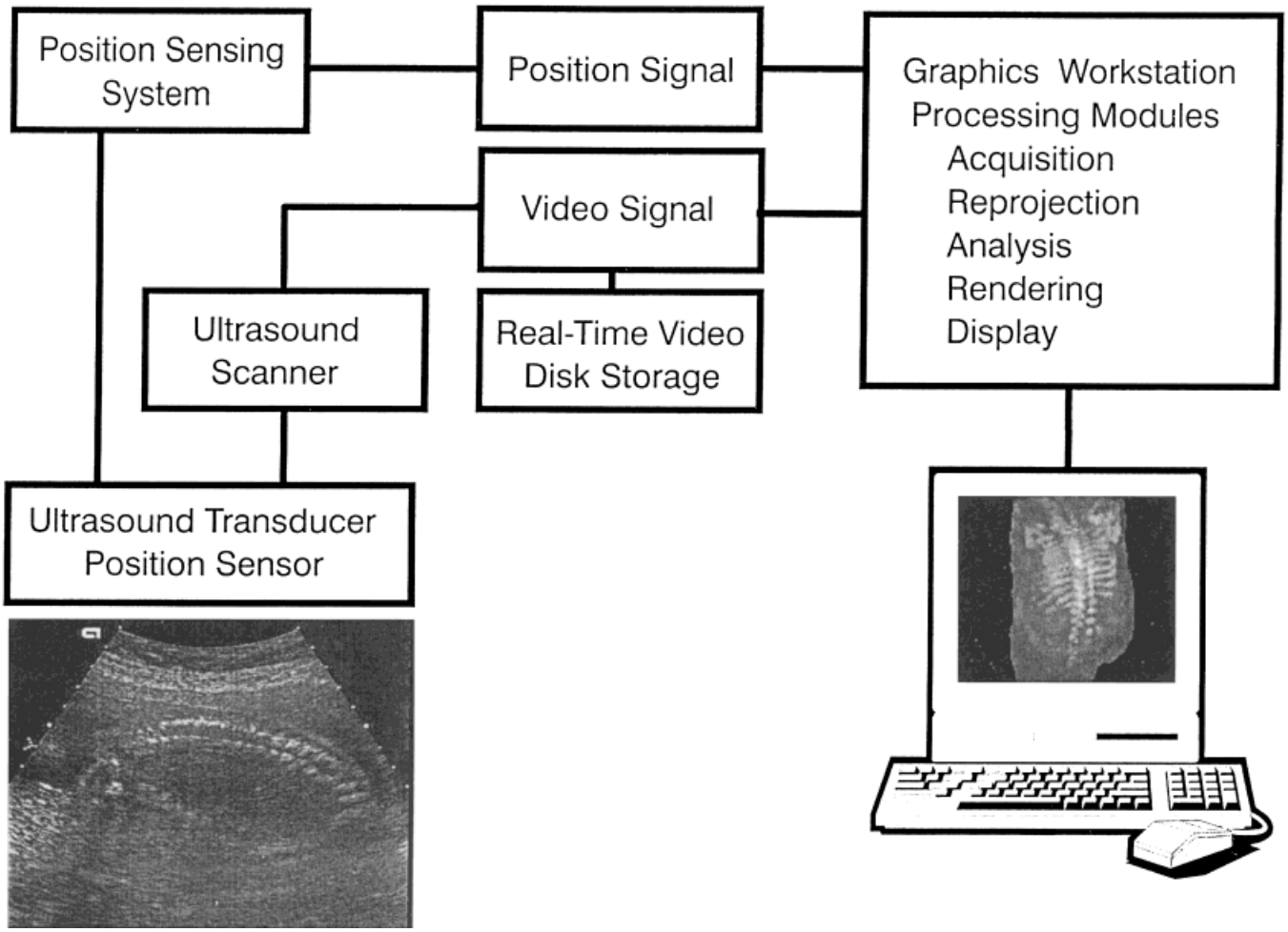


**Figure 1.** Block diagram of a volume sonographic imaging system. The primary components include a clinical scanning system, a position sensing system, and a graphics workstation.

in the scan coordinate system is calculated for each $B(x_i, y_i)$ using initial values for $[S(\theta_{1\,\mathrm{off}}, \theta_{2\,\mathrm{off}}, \theta_{3\,\mathrm{off}})]$ and position $[S(X_{\mathrm{off}}, Y_{\mathrm{off}}, Z_{\mathrm{off}})]$ based on physical measurements. The cumulative deviation error between each of the $B(X_i, Y_i, Z_i)$ balloon centers are computed, the offsets modified, and the error recomputed until the error reaches a minimum. Since by definition the balloon centers are located at the same position in the patient reference system, all $B(X_i, Y_i, Z_i)$ values should be the same and the error at a minimum when the correct offset values are determined. The process is repeated for each transducer and FOV and offset and scaling values saved in a calibration file. Transducer calibration need be performed only once or following a change in configuration of the position sensor attachment. The basic spatial relationships between the reference source, position sensor, and offsets are shown in Figure 4.

*4. Patient Image Acquisition.* Patient image acquisition is straightforward, and we have designed the system to permit the sonographer and physician to use conventional 2D scanning methods (Fig. 5). After the organ or area of interest is located by routine scanning and the image is optimized, the operator depresses a button on the scanner console for the duration of the volume acquisition; image and position data are acquired as the sonographer sweeps the transducer in a linear or rocking motion over the volume of interest. Upon button release the computer saves the data to disk and initializes the next patient data file automatically. In this manner, multiple volume acquisitions may be made rapidly and with minimal distraction to the operator and patient. Scan acquisition also may be initiated directly from the computer console. Two overlapping acquisitions can be combined into a single volume which is useful when imaging a large object. Patient scanning consists of making a series of volume ultrasound acquisitions (typically two to 10) during which gray-scale and color Doppler video image and position data are acquired into a graphics workstation using a slow sweep (5–15 s) through the anatomy of interest. Gray-scale and color data are separated during analysis as required. Depending on the type of patient study, images are acquired at either 10 or 30 frames/s and stored to disk.

### B. Ultrasound Data Analysis

*1. Sonographic Volume Reprojection.* Development of the volume data for an acquisition involves selecting the patient acquisition of interest, specifing the transducer, FOV, other parameters related to the image, and defining the acquisition limits and a region of interest. Currently, we specify the scan parameters (FOV, focus depth, frequency, etc.) manually, although it also is

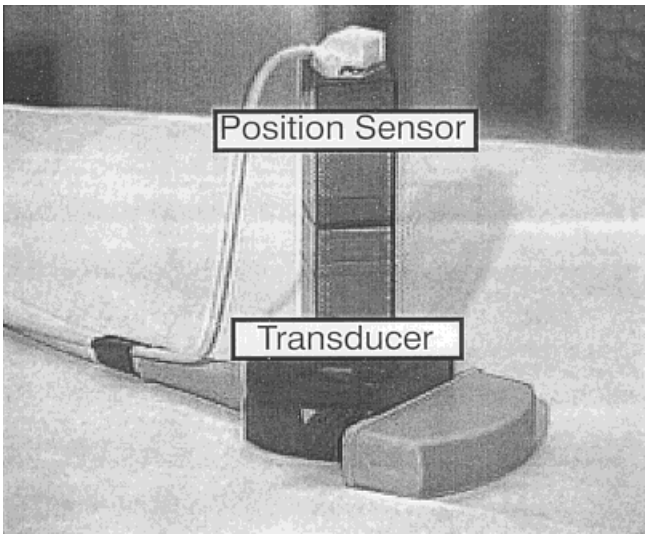


**Figure 2.** Image of transducer with positioner–scanning system. The offset between the transducer and sensor is to minimize interference. Other sensing systems are less susceptible to interference. Future systems could incorporate the sensor in the transducer assembly.

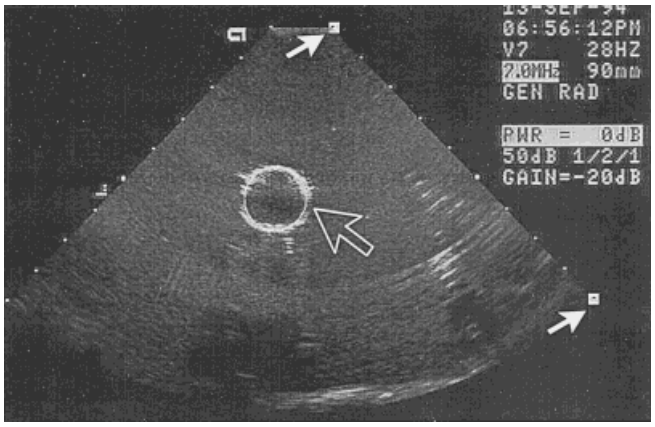


**Figure 3.** Image showing calibration image for a 7-MHz vector transducer. The pixel scaling information is determined by marking two depth markers (solid arrows) at a known separation and computing the pixel distance between them to obtain a pixel-per-centimeter scaling factor. System positioner to scan plane offsets are computed by determining the center of a spherical object by locating an interactive cursor over the circumference in each of multiple orientations. Since the same object is scanned, the center is fixed in all images. A minimum deviation algorithm is used to calculate the position sensor offset from the transducer scan plane.

possible to use character recognition algorithms to extract the necessary information automatically from the data text fields. Next, a region of interest is drawn around the anatomy of interest and the frames to be included in the reprojection identified by the operator. Our approach permits the operator to reproject the entire acquisition or select a subsegment for higher-resolution analysis. After the region of interest and range of images are selected, the computer determines the voxel scaling and offset factors for the volume matrix by incorporating the appropriate transducer calibration files. We create a cubic data matrix whose physical dimension is determined by the maximum extent of the data acquired. Thus, each volume has its own scaling factors and is standardized in terms of the number of voxels included. Typically, we use $128^3$ matrix as a standard but can increase or decrease the number of voxels depending on available memory and resolution requirements.

The basic pixel-to-voxel reprojection algorithm consists of converting each image pixel into a physical position and locating it in the volume at the proper position. Figure 6 shows the general algorithm used for pixel-to-voxel reprojection. The image intensity distribution consists of a spatial distribution of echo intensities at a given pixel location $P(X, Y, Z)$ (where $Z = 0$ in the image plane). The first step is to convert from a pixel image index location to a units of a physical measure (e.g., centimeters) $P(X_m, Y_m, Z_m)$, where $X_m = X \times SCALEX$, $Y_m = Y \times SCALEY$, and $Z_m = 0$. In general, $SCALEX$ and $SCALEY$ are equal. We add the position sensor offset values computed during calibration and setup to the image location $P(X_m, Y_m, Z_m)$ to obtain the position relative to the sensor $P(X_s, Y_s, Z_s)$ where $X_s = X_m + X_{\mathrm{OFF}}$; $Y_s = Y_m + Y_{\mathrm{OFF}}$; $Z_s = Z_m + Z_{\mathrm{OFF}}$. Next, we apply a rotation transformation $R(\theta_1, \theta_2, \theta_3)$ based on the relative angular orientation between the sensor position and the reference source to obtain the rotated pixel location $P(X_R, Y_R, Z_R)$. In addition, depending on which hemisphere the sensor is operating, the rotations will be performed in either a right- or left-handed coordinate system. At this point the pixel position has been referenced back to the sensor and we add the distance from the reference source to obtain the

**Table I.** Position system performance requirements.

| | Transducer Scanning Parameters | | |
|---|---|---|---|
| Frequency | 5.0 MHz | | |
| Lateral resolution | 0.5 mm | | |
| Axial resolution | 0.5 mm | | |
| Field of view | 100 mm | | |
| Plane thickness | 1.0 mm | | |
| | Positioning System Performance | | |
| | System Performance | Required at Resolution Limit | Required at 0.1 Resolution Limit |
| Range accuracy | 3.3 mm | 0.5 mm | 0.05 mm |
| Range resolution | 2.3 mm | 0.5 mm | 0.05 mm |
| Angular resolution | 0.35° | 0.29° | 0.03° |

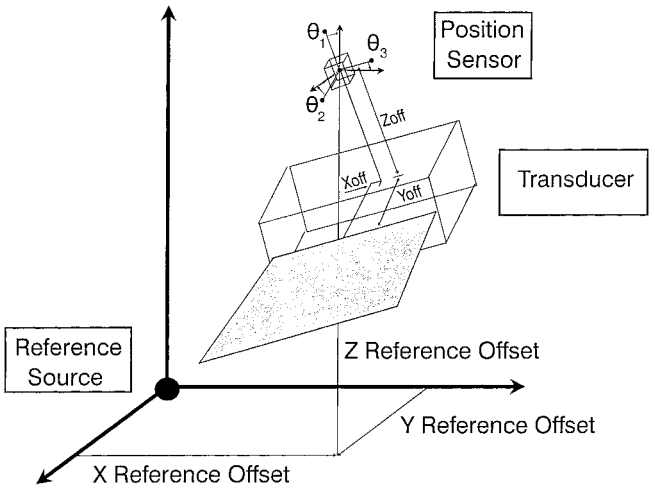


**Figure 4.** Diagram of the primary parameters used in computing the location of an image pixel in a volume referenced to a fixed location in the patient coordinate system. The position sensor provides a relative *X*, *Y*, and *Z* distance from the source plus three rotation angles ($\theta_1$, $\theta_2$, $\theta_3$) referencing the relative orientation between the source and the sensor. The source field pattern results in two symmetric hemispheres requiring either right- or left-hand coordinate transformations, depending on the relative orientation of the system. Transducer scan plane, image, and position sensor offsets are also necessary to locate an image pixel in the patient coordinate system.

volume position $P(X_V, Y_V, Z_V)$, where $X_V = X_R + X_{REF}$; $Y_V = Y_R + Y_{REF}$; $Z_V = Z_R + Z_{REF}$. Pixels from different images that correspond to the same voxel are evaluated by either selecting the maximum voxel to retain or averaged. Selecting the maximum voxel minimizes the effects of shadowing and dropout at the cost of a slight increase in image noise. The reprojection process results in all voxels being directly referenced to a fixed point in the patient coordinate system as established by the source transmitter. A calibration file records all reprojection, scaling, and transducer

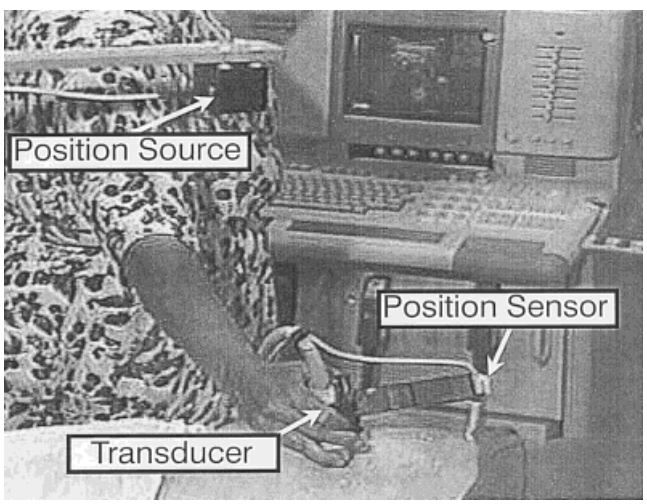


**Figure 5.** Image of the overall system in operation during a typical clinical scan. The source assembly is visible at the top of the image. The transducer and position sensor are located on the patient. The source also could be positioned under the table.

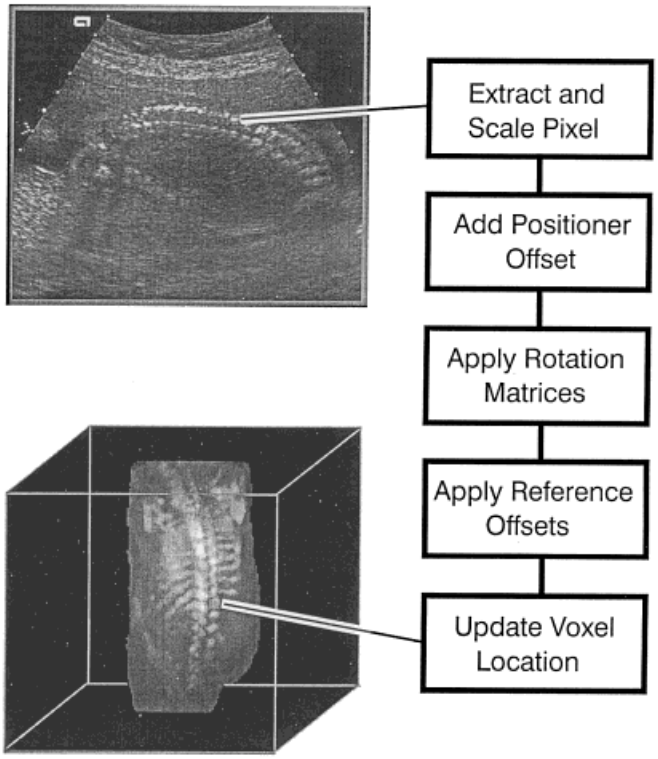


**Figure 6.** A block diagram of the basic reprojection algorithm for mapping a pixel in the sonographic image to a volume data matrix.

parameters. Table II shows an example of the calibration information saved for a volume data set. Color Doppler data are reprojected with grayscale data and extracted during volume rendering [34]. Typical volume data storage requires 2 Mbytes for grayscale and 6 Mbytes for color data for a $128^3$ data set.

*Physiologic Synchronization.* Cardiac or blood flow imaging must be synchronized to the cardiac cycle by first determining the heart rate and the corresponding parts of the cardiac cycle. In these cases a box, or region of interest, is drawn over the heart or vessel. A temporal Fourier transform of the acquired image series for each point in the region of interest is made to evaluate the regularity of the heart rate and determine the location of common points in the cardiac cycle (Fig. 7) [35,36]. Ectopic or irregular heartbeats can be eliminated from the study analysis. End-diastolic times are used to assign each acquired image to the proper point in the cardiac cycle. Subsequently, a region of interest is drawn including the heart and vessels of interest. As described above each image is reprojected with scaling factors into one of a series of volume data sets (currently up to 16 volumes/cardiac cycle) corresponding to the appropriate time in the cardiac cycle. Cardiac data sets require 33 Mbytes for gray-scale data and 100 Mbytes for color data.

*2. Sonographic Volume Augmentation and Filtering.* Depending on the FOV and the rate of scanning, most volume data will have small gaps where no scan data were obtained. This situation can be corrected by two methods: either by acquiring very slowly and oversampling the volume of interest or by augmenting the data volume to fill in the gaps using a variety of estimation methods. Acquiring images slowly generates large amounts of data and requires long scanning times, both of which

**Table II.** Volume reprojection parameters

| 2D ultrasound image-scaling calibration | | | |
|---|---|---|---|
| Image distance calibration | 0.030 cm/pixel | | |
| Transducer positioner calibration | | | |
| Transducer position offsets | $x$: 5.71 cm | $y$: 0.13 cm | $z$: 11.30 cm |
| Transducer angle offsets | $\theta_1$: 0.1° | $\theta_2$: −0.1° | $\theta_3$: − 0.4° |
| Center of image (pixel) | 290.5 | | |
| Invert status | Noninvert | | |
| Field of view | 100.0 mm | | |
| Rotation system | Left-hand rule | | |
| Volume reprojection parameters | | | |
| Voxel dimensions (side) | 0.672 cm/voxel | | |
| Total volume scanned | 637.25 $cm^3$ | | |
| Volume offsets (from reference) | $x$: −27.3 cm | $y$: 8.11 cm | $z$: 25.87 cm |
| Volume rotation | $\theta_1$: 0.0° | $\theta_2$: 0.0° | $\theta_3$: 0.0° |
| Filter status (if used) | Median | 3 pt kernel | |
| No. of images (if gated) | 13 (gated study) | | |

are often impractical in a clinical environment. We use an algorithm that incorporates nearest-neighbor information to estimate the proper voxel value. The algorithm successively reduces the matrix resolution by factors of 2 (e.g., 128 → 64 → 32 → 16 → 8 → 4) and replaces gaps with a valid voxel from the next lowest resolution. If there is a gap at the next lowest resolution, the process continues until a valid voxel is found. By performing the process recursively large gaps in the volume can be filled in with minimal compromise in data quality (Fig. 8).

After volume data are augmented they may be filtered depending on the quality of the data and the diagnostic question. We typically use either a $3 \times 3 \times 3$ Gaussian or median filter to improve the spatial coherence and signal-to-noise ratio. In general, a median filter provides better results than a Gaussian filter, particularly for reducing speckle noise while preserving resolution [37]. Synchronized cardiac data for the entire cardiac cycle are filtered using similar methods.

*3. Sonographic Volume Data Measurement.* Volume data provide the opportunity to obtain quantitative data regarding organ size and volume. Volume measurement is accomplished by masking using either individual planes masks or a volume interactive electronic scalpel so that the region of interest contains only the object of interest. After the object is masked the voxels are summed and the matrix voxel scaling factors applied to determine the volume. This approach permits measurement of regular, irregular, and disconnected objects with equivalent accuracy. Our calibration methods permit measurement of distance and volume with an accuracy of better than 5% for regular and irregular objects and in vivo organs [33,38,39]. Our data show that the percent error is relatively independent of the object size over several orders of magnitude. For small objects in which machine resolution is significant, factor errors will increase accordingly. The absolute error will vary with the volume of the object and the size of the voxel. A larger FOV will result in larger voxels for the same matrix size with a corresponding increase in the absolute error. In general, the improved measurement accuracy afforded by volume sonographic methods makes possible accurate quantitative measurement of heart chambers, vessel dimensions, and organ volumes.

*4. GUI.* Accurate interpretation of patient data requires that features be recognizable rapidly and that the operator be able to optimize the viewing orientation for the best presentation of anatomy. To facilitate usage in a clinical environment we have developed an intuitive, easy-to-use GUI with a rapid learning curve that facilitates physician operation of the system. An intuitive GUI is essential to physician acceptance and use of computer graphics systems. Our GUI is based on a layered system whereby the operator selects a patient and data volume for evaluation. Next, a selection of options provides access to acquisition, reprojection, processing, and viewing modules. The specific modules available depends on the type of study and previous analysis. Figure 9 shows several layers of the system. Each module accesses the data volume and scaling data and performs the desired operation. Single or multiple display windows are used depending on the module. The entire GUI is operated by the mouse and does not require operator keyboard data entry with the exception of entering new patients' names. The GUI incorporates an interactive volume renderer that permits optimization of viewing orientation and data presentation by permitting the viewer to select among various processing functions including rotation, reslicing, and volume rendering, stereoviewing (Fig. 10). The GUI is written in Xlib and Xview and provides a flexible platform for development. New modules may be added easily to accomodate additional processing functions.

*5. Sonographic Volume Data Review.* Volume data review typically begins with reslicing of the data volume to find the optimum viewing plane. Cut planes can be viewed for any orientation and position in the anatomy of interest. We simultaneously display three intersecting orthogonal views through a common point selected by the viewer for comparison and localization pur-

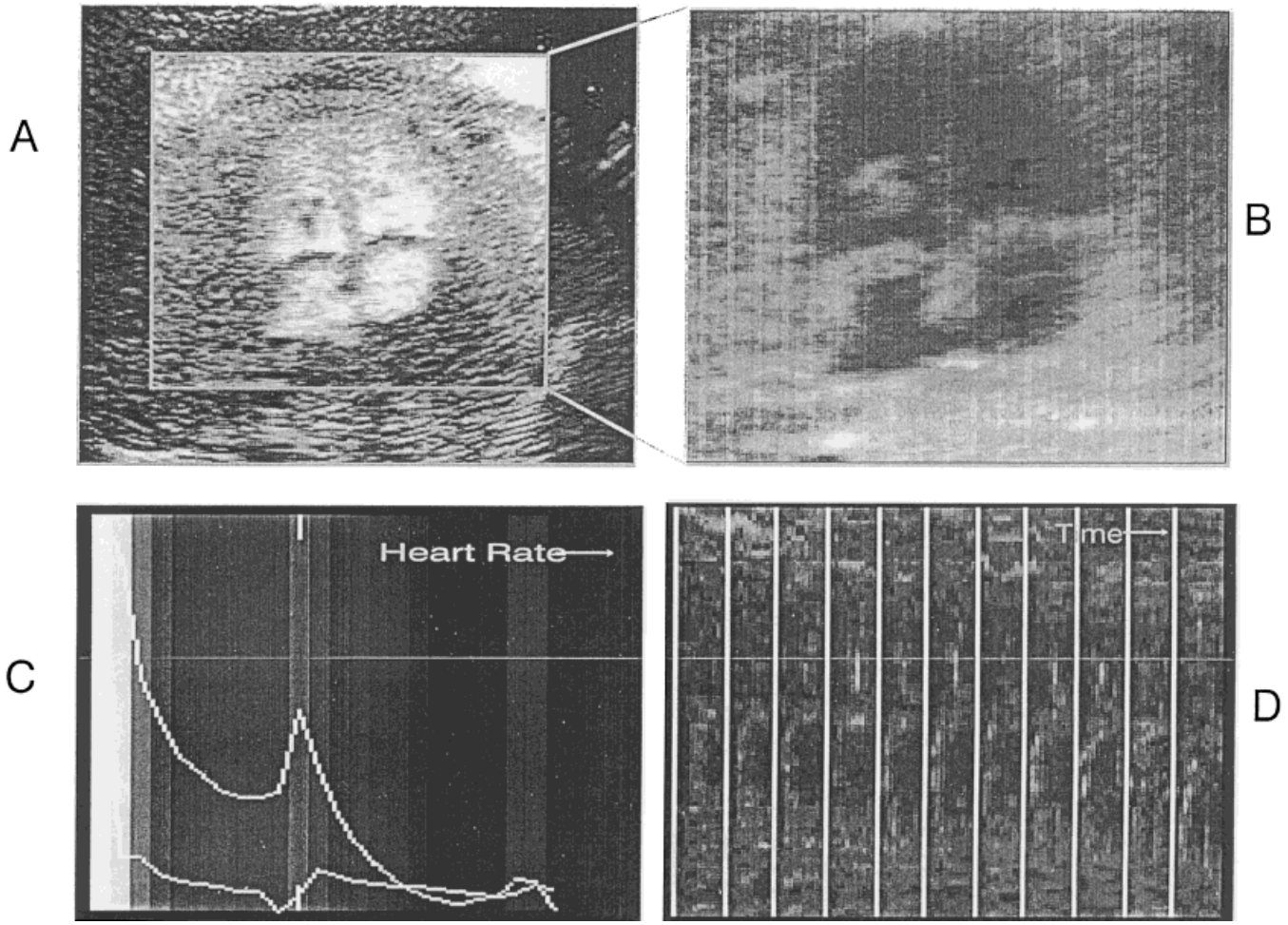


**Figure 7.** Algorithm for determining the location of common points of the cardiac cycle. A temporal Fourier transform is made for all the points in the square region of interest covering the heart (A). The resulting Fourier magnitude image (B) shows the location of nonzero periodic intensity variations in the image acquisition. The temporal Fourier transform for all of the pixels is summed to produce a composite measure of cardiac motion (C) and determine the heart rate automatically. Inversion of the beat frequency data from the Fourier transform is used to obtain zero-crossing times and produce a synchronization map for the entire acquisition (D).

poses. The volume can be examined by scrolling through parallel planes from the initial orientation including orthogonal planes. Scolling also can be repeated after rotating the volume to a more optimal orientation. We have found that viewer comprehension is improved by reorienting volume data to a standard anatomic orientation to provide consistency between patients and analysis methods.

Also, we use volume-rendering methods to display the entire volume in a single image. Our primary volume-rendering approach is a modification of ray casting [11] to accomodate the challenges of ultrasound data. The method is either a modified maximum intensity projection (MIP) or variable transparency projection with depth shading. Rendering is particularly valuable for viewing color Doppler blood flow data that may be either shown with gray-scale data or after extraction from the data volume to display the isolated vascular anatomy. Using the interactive renderer the viewer may interactively rotate and zoom the data volume to optimize the display orientation. Target organ visualization is further enhanced using a 3D electronic scalpel we have developed to interactively extract tissues or organs of interest from the rest of the volume scanned [40]. Using the electronic scalpel, the viewer may slice away sections of the data volume to isolate the anatomy of interest rather than using slower single-plane masking techniques. Also, we use interactive stereoviewing with all studies, which has proven essential to improve user comprehension of complex anatomic structures. Currently, we use liquid crystal display (LCD) glasses synchronized to the display monitor, although we continue to explore other options such as holography.

Cardiac data are displayed as a dynamic sequence on the graphics display system. This display is similar to the cine-loop displays provided on clinical ultrasound systems, but has a significant difference in that dynamic volume data are displayed interactively so that the viewing orientation and plane may be changed to observe the dynamics and anatomy from different orientations throughout the cardiac cycle, permitting the viewer to optimize the desired plane or angle of viewing. The display frame rate can be varied so that each frame may be evaluated separately or as a cine display. In addition, views that optimize display of the valve planes may be made to provide an assessment

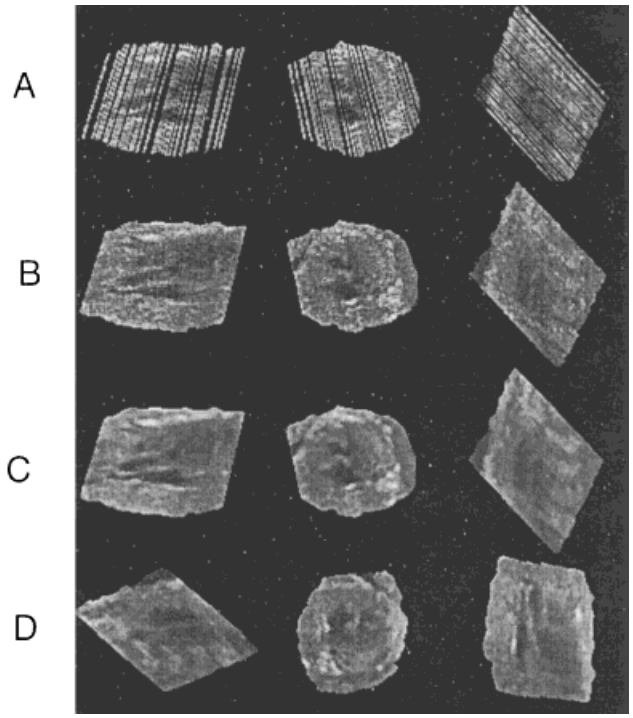


**Figure 8.** Reprojected volume data may have gaps due to scanning rapidly (A). An augmentation program using nearest neighbors is used to fill in any gaps (B). A $3 \times 3 \times 3$ median filter is used to reduce noise in the image (C) and the volume data are reoriented to a standard anatomic position (D).

of valve function. All volume data can be displayed using stereographic methods as part of the interactive data review.

## III. EXAMPLES OF CLINICAL STUDIES

Routine clinical scanning using a conventional real-time scanning transducer with integrated position sensor is straightforward and rapid, requiring typically $<30$ s/scan acquisition. Reprojection requires between 0.5 and 5 min, depending on the acquisition length and complexity. For example, cardiac dynamic studies require more analysis than static volume acquisitions. Interactive volume display is available within 10 s. Quantitative data are available for measuring length, area, and volume using interactive tools with accuracy established over a volume range of 10–2400 ml [33].

Clinical imaging trials have been under way in several areas ranging from obstetric to vascular studies. This section presents some examples of the results obtained with the system described above [10,12,41,42]. The images of the hepatic vessels (Fig. 11) and maternal–fetal placental vessels (Fig. 12) were produced from an acquisition of approximately 20 s in normal volunteers and were obtained without contrast material [34]. The fetal skull (Fig. 13) was acquired in approximately 20 s as part of a complete acquisition of the entire fetus and uterine contents. The skull could be evaluated in more detail owing to the inclusion of the entire skull in a single image rather than a single plane [42]. Fetal cardiac function in a 32-week fetus can be evaluated as a series of volume data sets throughout the cardiac cycle and reviewed as a dynamic display from multiple orientations and with the chambers extracted (Fig. 14) [35]. A typical gated cardiac acquisition requires 30 s and does not require an electrocardiographic signal. These examples demonstrate the capabilities of volume sonography imaging to produce high-quality volumetric data from a variety of patients in a rapid manner to evaluate tissue signature and structure in addition to blood flow.

**A. Optimization of Sonographic Volume Data Visualization.** Determination of the optimal visualization method for volume sonography is challenging, since image data are generally difficult to threshold or segment, because different tissues often have similar intensities with only the interface being visible [11]. As a result, an important part of visualization is the ability to review patient data interactively, including the flexibility to rotate, scale, and view objects from perspectives that optimize visualization of the anatomy of interest, which requires high-performance viewing stations. Viewing with stereographic viewing appears to be of clinical value to enhance visualization. Physician involvement in optimizing and enhancing visualization tools is essential in the ongoing evaluation of these techniques.

Thus far, we have found that several visualization methods are useful for volume data analysis. Viewing planar slices from arbitrary orientations is a straightforward method of volume display for interactive review that closely resembles current clinical scanning procedures. In addition, planar slicing of the volume offers projections not available during sonogram acquisition. Our experience has shown that intermediate processing or filtering of ultrasound image data may be helpful, but is not necessarily required to review volume data.

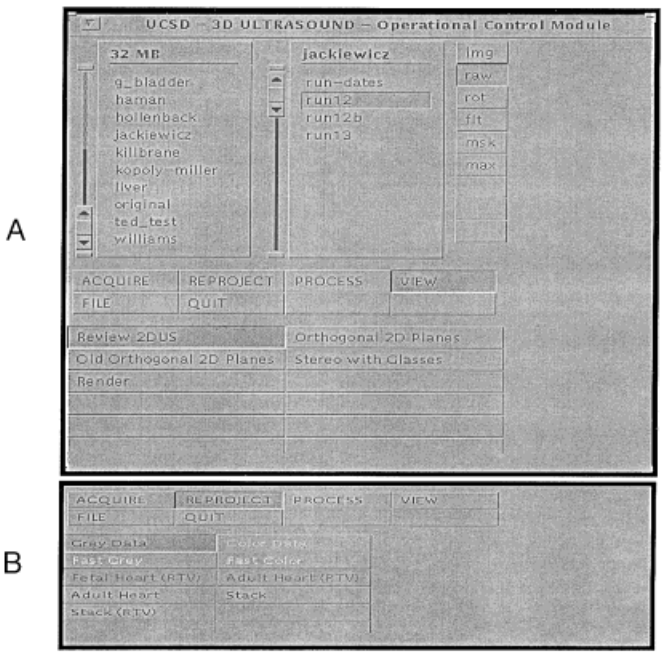


**Figure 9.** The main page of the graphical user interface (GUI) used for control of patient selection, acquisition, reprojection, processing, and viewing functions. (A) Patient selection with a summary of different acquisitions and the type of files available for a given acquisition. The lower part shows selections for the view option. The specific options will vary depending on the type of acquisition (e.g., gray, color, cardiac). (B) Selections for the reproject option. Acquisitions may be reprojected using different options depending on the requirements such as color, gating, and single or multiple volumes.

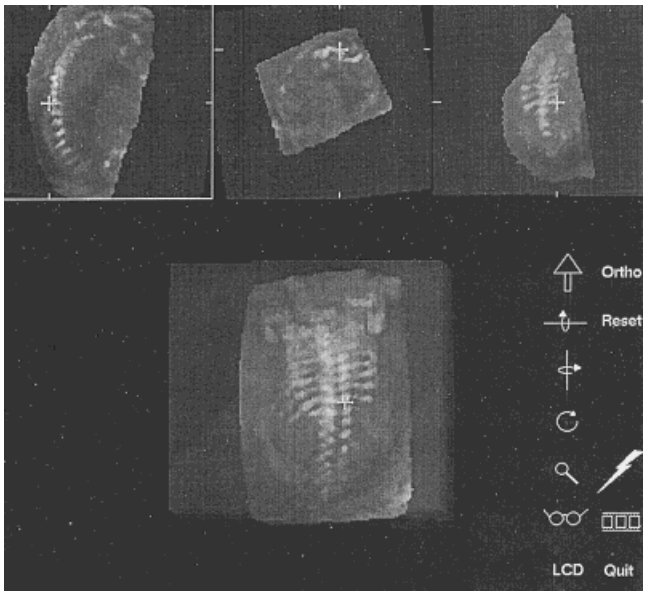


**Figure 10.** An image of the display from our interactive renderer showing the subfunctions of the renderer. The upper panels show orthogonal slices from the volume. The white cross is the point of common intersection between planes. Each plane will reflect rotation of the entire rendered volume under interactive control using the icons in the lower right image. The volume-rendered data are visible in the main lower center screen. The white square is common to the cross in the upper images. The icons on the lower right panel represent the following functions: large arrow = scroll in/out in current selected plane image; three circular arrows = rotation of rendered volume in indicated direction (direction changes by using right/left mouse button); magnifying glass = zoom/reduction of rendered image; glasses = stereo view using either red/green or LCD glasses; ortho = show/hide orthogonal intersecting planes; lightning bolt = volume editing tool to remove highlighted regions in volume rendered image; film clip = show last rotation function as continuous update of motion.

Surface-fitting provides for rapid evaluation of the overall surface features of the object. However, surface-fitting is sensitive to noise and a distinct interface (e.g., fluid–tissue) is necessary. These methods will most likely be used in specialized applications such as vascular or obstetric imaging.

Volume-rendering methods using ray-casting and splatting approaches produce high-quality images that are relatively tolerant of noise in the ultrasound data [11]. Filtering can improve results as long as fine detail is not obscured. Careful selection of opacity values is important to provide an accurate rendition of the structure being studied. Transparency permits viewing surface and subsurface features that can be helpful in establishing spatial relationships. For specific applications, maximum-intensity methods give a clear view of structures such as bones in the hands, spine, or ribs, although they are often best applied to selected regions of the volume.

Animation sequences such as rotation and gated cine-loop review greatly assist volume visualization. Without the animation display of rendered volumetric images offered by real-time processing or precalculation, the physician often has a difficult time extracting 3D information from 2D displays.

The principal challenges to acquiring an acceptable volume data set have been patient motion, organ position, and patient habitus. Since acquisition time is relatively quick, we can begin a new acquisition as soon as the motion has stopped. Our experience shows several acquisitions may be made without significant motion during the study. Furthermore, areas of acoustic shadowing or attenuation which are common in ultrasound imaging do not compromise other areas of the acquisition, thus permitting use of segments of the acquisition that are nonmoving or otherwise well visualized. In addition, organ orientation and position may not allow for specific images to be obtained in 2D; it is as yet unknown how often volume data will allow for those images to be obtained and to determine which will be clinically relevant. Clinical experience with volume sonographic imaging has demonstrated the potential of the technique with different systems emphasizing different capabilities. While the ultimate clinical impact remains to be determined, results to date have been encouraging and the number of published papers are increasing yearly.

Analysis techniques used with 3D ultrasound data enhance the visibility of anatomy; however, we have found that optimal visualization depends on several factors: First, the overall image quality of the 2D ultrasound images directly affects the quality of the volume images. The distance between the structure and the transducer may lead to one side of the anatomy being imaged more clearly than the other side. Second, acquisition of 2D ultrasound images may be better in one plane than others, owing to the thickness of the ultrasound scan plane. Third, rendered image quality is affected by the anatomic orientation and beam pathway. Signal dropout from shadowing due to overlying structures can significantly obscure structural detail. Compounding data obtained from different orientations can minimize the adverse effects of signal dropout, although elastic deformation of tissues due to pressure from the transducer during scanning can distort and complicate realignment of scans. Fourth, as already noted, additional volume acquisitions are necessary when the patient moves during a scan. Fifth, faster hardware is needed, and is becoming affordable, to shorten the time between acquisition and display. Currently, the time required for volume sonography can be broken down as follows: scan 10–30 s, reprojection 0.5–2 min (gated cardiac 2–10 min), rendering 0.5–1 s/view, although recently we have demonstrated real-time rendering on more recent hardware. In the future we anticipate reducing time from acquisition to display to $<10$ s, which will greatly enhance clinical acceptance. As experience with 3D ultrasound increases, continued refinement of analysis and visualization software will further assist in making a more accurate diagnosis.

An important part of sonographic visualization is the inter-

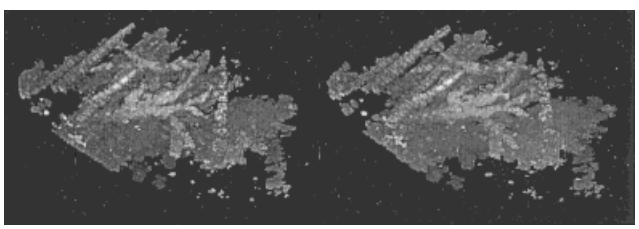

**Figure 11.** A stereo image pair from a color Doppler energy (CDE) acquisition from a liver in a normal volunteer. The color velocity data has been extracted from the volume and rendered using the interactive renderer shown in Figure 10. The full gray-scale and color data are viewable in the orthogonal planes.

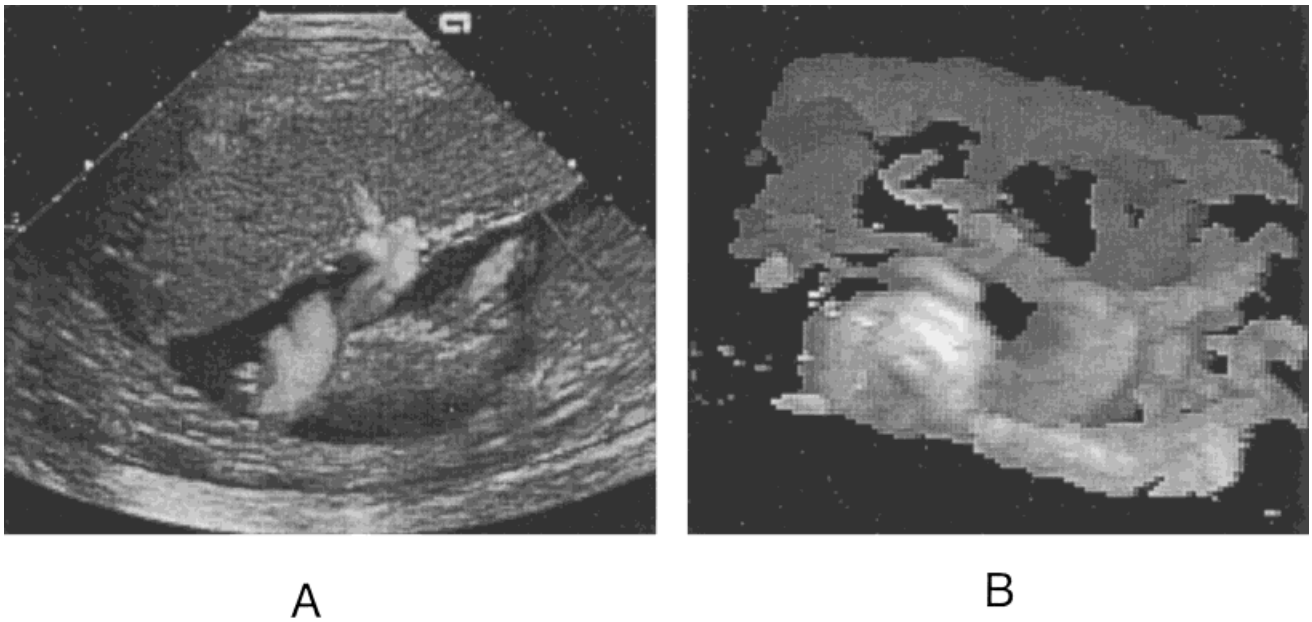


**Figure 12.** (A) A 2D CDE scan of a 26-week uterus showing the insertion of the umbilical cord from the fetus into the placenta. (B) Volume-rendered display of the same data showing the improved visualization resulting from using all the velocity data. The viewer can interactively rotate and zoom the image to optimize the vantage point.

active capability of the viewing station. Because of the computationally intensive nature of many visualization algorithms, either high-performance computing or precalculation is required. Review of patient data must include the flexibility to rotate, scale, and view objects from perspectives that optimize visualization of the anatomy of interest. Stereographic viewing also is of clinical value to enhance visualization, although more detailed studies are needed to establish its clinical impact.

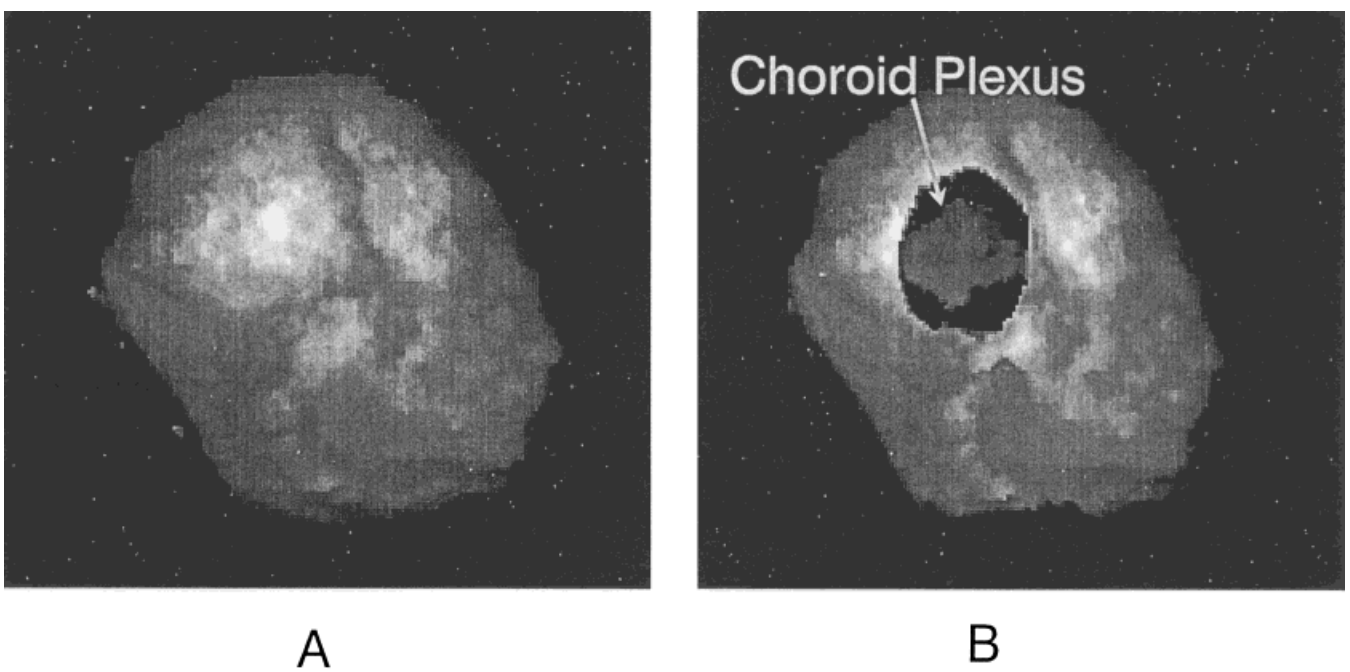


**Figure 13.** A volume-rendered skull from an 18-week fetus showing the primary cranial sutures (A). (B) The same image after using the electronic scalpel to remove those portions of the skull closest to the observer to reveal the choroid plexus inside the cranial vault. Removal of the overlying skull was performed on the volume-rendered image in $<$10 s.

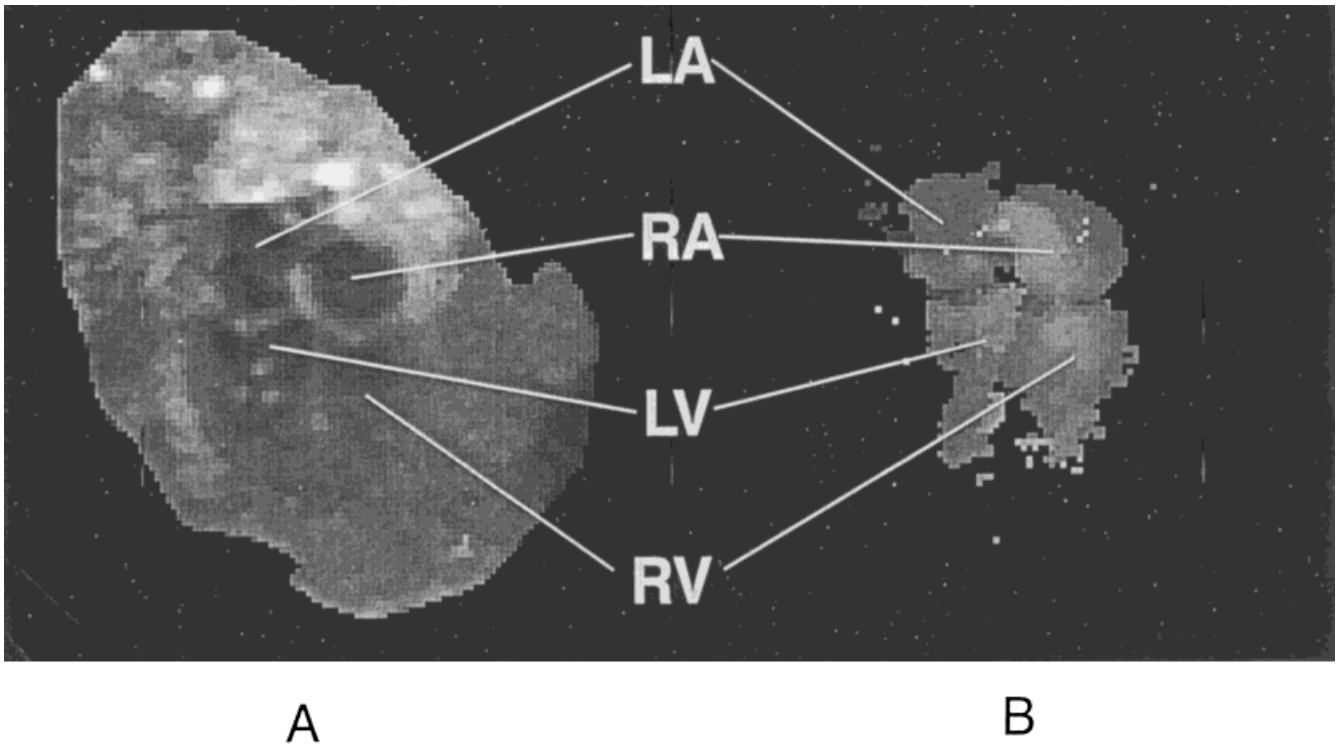


**Figure 14.** (A) A single slice reproducing the four-chamber view of a 32-week fetal heart. The four chambers are identified. Other structures including the valves, foramen ovale, and papillary muscles are clearly visible. The data may be displayed as dynamic sequence to show the heart motion. (B) A volume-rendered image of the blood pool for the data shown in (A). The four chambers are clearly visible as are the valve planes and intracardiac septa. The data may be rotate as well as viewed dynamically to fully appreciate the anatomy and function of the heart.

## IV. CONCLUSIONS

Sonographic volume imaging, an area undergoing rapid development, represents a natural extension of conventional sonography that requires integrating a series of 2D image slices to develop a 3D impression of underlying anatomy or pathology. Preliminary work has shown that 3D visualization can enhance the diagnostic process by providing better delineation of complex anatomy and pathology. Interactive manipulation of images by rotation and zooming in on localized features or isolating cross-sectional slices can assist interpretation by physicians and allow for quantitative measurement of volume or area.

Our experience has shown that an interactive approach means clinically that images of anatomy and organs can be displayed in an intuitively straightforward manner, so that the physician feels as if he is holding a model of the organ in his hands, allowing him to ''see'' the organ as it actually is. Using our methods, ultrasound data can be thought of as a volume with which the clinican rapidly interacts as though exploring internal patient anatomy directly, rather than a series of 2D images viewed in real time or statically. However, interactivity requires affordable high-performance computer graphics systems to assist physicians in comprehending patient anatomy and injury and quickly extract vital information. Without interactive capability 3D methods can be more time consuming than current clinical methods, thus limiting their clinical utility.

Our methodology could be integrated with existing sonographic equipment at modest cost ($40,000/unit, based on projected future cost per performance improvements), thus facilitating wide distribution of this technique. Acquisition of volume patient data also affords the possibility of review after the patient has left the medical facility, or communication of the entire volume via an interactive communications link to a specialist at a tertiary care center. This could reduce the need to refer a patient to a specialized center, by permitting the primary physician and the specialist to consult and interactively review the study from both sites, thus improving patient care and reducing costs. In addition, network review of volume data could reduce the operator dependence for patient scanning. Ultimately, an improved understanding of patient anatomy offered by 3D ultrasound imaging may make it easier for primary care physicians to understand complex patient anatomy. Access to volume data at specialization centers may afford more sophisticated analysis and review, further augmenting patient diagnosis and treatment.

## ACKNOWLEDGMENTS

This work was supported in part by gifts and grants from the ACUSON Corporation. The authors acknowledge the assistance of Thomas Davidson in software development.

## REFERENCES

1. K. Baba, K. Satch, S. Sakamoto, T. Okai, and I. Shiego. ''Development of an ultrasonic system for three-dimensional reconstruction of the fetus,'' *J. Perinat. Med.* **17,** 19–24 (1989).
2. M. Belohlavek, D. A. Foley, T. C. Gerber, T. M. Kinter, J. F. Greenleaf, and J. B. Seward. ''Three- and four-dimensional cardiovascular ultrasound imaging: A new era for echocardiography,'' *Mayo Clin. Proc.* **68,** 221–240 (1993).
3. D. R. Fulton, G. R. Marx, N. G. Pandian, et al. ''Dynamic three-

dimensional echocardiographic imaging of congenital heart defects in infants and children by computer-controlled tomographic parallel slicing using a single integrated ultrasound instrument,'' *Echocardiography* **11,** 155–164 (1994).
4. J. F. Greenleaf, M. Belohlavek, T. C. Gerber, D. A. Foley, and J. B. Seward. ''Multidimensional visualization in echocardiography: An introduction,'' *Mayo Clin. Proc.* **68,** 213–220 (1993).
5. U. M. Hamper, V. Trapanotto, S. Sheth, M. R. DeJong, and C. I. Caskey. ''Three-dimensional US: Preliminary clinical experience. *Radiology* **191,** 397–401 (1994).
6. D. L. King, D. L. King, and M. Y. Shao. ''Three-dimensional spatial registration and interactive display of position and orientation of real-time ultrasound images,'' *J. Ultrasound Med.* **9,** 525–532 (1990).
7. H. C. Kuo, F. M. Chang, C. H. Wu, B. L. Yao, and C. H. Liu. ''The primary application of three-dimensional ultrasonography in obstetrics,'' *Am. J. Obstet. Gynecol.* **166,** 880–886 (1992).
8. W. R. Lees, J. E. Gardener, and A. Gillams. ''Three dimensional ultrasound of the fetus,'' *Radiology* **181,** 131–132 (1991).
9. R. A. Levine, A. E. Weyman, and M. D. Hanschumacher. ''Three-dimensional echocardiography: Techniques and applications,'' *Am. J. Cardiol.* **69,** 121H–130H (1992).
10. T. R. Nelson and D. H. Pretorius. ''Three-dimensional ultrasound of fetal surface features,'' *Ultrasound Obstet. Gynecol.* **2,** 166–174 (1992).
11. T. R. Nelson and T. T. Elvins. ''Visualization of 3D ultrasound data,'' *IEEE Comput. Graph. Appl.* **13,** 50–57 (1993).
12. D. H. Pretorius, T. R. Nelson, and J. S. Jaffe. ''Three-dimensional sonographic analysis based on color flow Doppler and gray scale image data: A preliminary report,'' *J. Ultrasound Med.* **11,** 225–232 (1992).
13. R. N. Rankin, A. Fenster, D. B. Downey, P. L. Munk, M. F. Levin, and A. D. Vellet. ''Three-dimensional sonographic reconstruction: techniques and diagnostic applications,'' *AJR* **161,** 695–702 (1993).
14. H. Selzer, P. L. Lee, J. Y. Lai, and H. J. Frieden. ''Computer-generated three-dimensional ultrasound images of the carotid artery,'' *Comput. Cardiol.* 21–26 (1988).
15. J. F. Brinkley, S. K. Muramatsu, and W. D. McCallum. ''In vitro evaluation of an ultrasonic three-dimensional imaging and volume system,'' *Ultrason. Imaging* **4,** 126 (1982).
16. D. L. King, D. L. King, and M. Y. Shao. ''Evaluation of in vitro measurement accuracy of a three-dimensional ultrasound scanner,'' *J. Ultrasound Med.* **10,** 77–82 (1991).
17. M. H. Halliwell, H. Key, D. Jenkins, P. C. Jackson, and P. N. T. Wells. ''New scans from old: Digital reformatting of ultrasound images,'' *Br. J. Radiol.* **62,** 824–829 (1989).
18. W. R. Lees, R. Balen, C. M. Allen, and D. Kessel. ''Diagnostic value of 3D tumor blood flow maps derived from Doppler data,'' *Radiology* **193,** 335–336 (1994).
19. K. J. Ng, J. E. Gardener, D. Rickards, W. R. Lees, and E. J. Milroy. ''Three-dimensional imaging of the prostatic urethra—an exciting new tool,'' *Br. J. Urol.* **74,** 604–608 (1994).
20. P. Lyden and T. R. Nelson. ''Visualization of the cerebral circulation using 3D transcranial power doppler ultrasound,'' *J. Neuroimag.* (in press).
21. P. L. Carson, D. D. Adler, J. B. Fowlkes, K. Harnist, and J. Rubin. ''Enhanced color flow imaging of breast cancer vasculature: Continuous wave Doppler and three-dimensional display,'' *J. Ultrasound Med.* **11,** 377–385 (1992).
22. D. Rotten, J. M. Levaillant, E. Constancis, A. Collet-Billon, Y. LeGuerine, and P. Rua. ''Three-dimensional imaging of solid breast tumors with ultrasound: Preliminary data and analysis of its possible contribution to the understanding of the standard two-dimensional sonographic images,'' *Ultrasound Obstet. Gynecol.* **1,** 384–390 (1991).
23. A. Salustri and J. R. Roelandt. ''Ultrasonic three-dimensional reconstruction of the heart,'' *Ultrasound Med. Biol.* **21,** 281–293 (1995).
24. J. B. Seward, M. Belohlavek, P. W. O'Leary, D. A. Foley, and J. F. Greenleaf. ''Congenital heart disease: Wide-field, three-dimensional, and four-dimensional ultrasound imaging,'' *Am. J. Cardiac Imag.* **9,** 38–43 (1995).
25. A. Lee, J. Deutringer, and G. Bernaschek. ''Voluvision: Three-dimensional ultrasonography of fetal malformations,'' *Am. J. Obstet. Gynecol.* **170,** 1312–1314 (1994).
26. H. Steiner, A. Staudach, D. Spinzer, and H. Schaffer. ''Three-dimensional ultrasound in obstetrics and gynaecology: Technique, possibilities and limitations,'' *Hum. Reprod.* **9,** 1773–1778 (1994).
27. E. Merz, F. Bahlmann, and G. Weber. ''Volume scanning in the evaluation of fetal malformations: A new dimension in prenatal diagnosis,'' *Ultrasound Obstet. Gynecol.* **5,** 228–232 (1995).
28. D. H. Pretorius, M. H. House, T. R. Nelson, and K. A. Hollenbach. ''Evaluation of normal and abnormal lips in fetuses: Comparison between three- and two-dimensional sonography,'' *AJR* **165,** 1233–1237 (1995).
29. D. H. Pretorius and T. R. Nelson. ''Fetal face visualization using three-dimensional ultrasonography,'' *J. Ultrasound Med.* **14,** 349–356 (1995).
30. E. A. Geiser, L. G. Christie, D. A. Conetta, C. R. Conti, and G. S. Gossman. ''A mechanical arm for spatial registration of two-dimensional echocardiographic sections,'' *Catheter. Cardiovasc. Diagn.* **8,** 89–101 (1982).
31. T. C. Hodges, P. R. Detmer, D. H. Burns, K. W. Beach, and D. E. Strandness. ''Ultrasonic three-dimensional reconstruction: In vitro and in vivo volume and area measurement,'' *Ultrasound Med. Biol.* **20,** 719–729 (1994).
32. F. H. Raab, E. B. Blood, T. O. Steiner, and H. R. Jones. ''Magnetic positioning and orientation tracking system,'' *IEEE Trans. Aerospace Electronic Systems* **15,** 709–717 (1979).
33. M. Riccabona, T. R. Nelson, D. H. Pretorius, and T. E. Davidson. ''Distance and volume measurement using three dimensional ultrasound,'' *J. Ultrasound Med.* **14,** 881–886 (1995).
34. D. H. Pretorius, T. R. Nelson, R. Baergen, and C. Cantrell. ''3-Dimensional ultrasound and power doppler imaging of placental vasculature,'' *Acad. Radiol.* **2,** 1154 (1995).
35. T. R. Nelson, D. H. Pretorius, M. Sklansky, and S. Hagen-Ansert. ''Three-dimensional echocardiographic evaluation of fetal heart anatomy and function: Acquisition, analysis and display,'' *J. Ultrasound Med.* **15,** 1–9 (1996).
36. T. R. Nelson. ''Synchronization of time-varying physiological data in 3DUS studies,'' *Med. Physics* **22,** 973 (1995).
37. T. R. Nelson and D. H. Pretorius. ''3D ultrasound image quality improvement using spatial compounding and 3D filtering,'' *Med. Phys.* **21,** 998–999 (1994).
38. T. R. Nelson and D. H. Pretorius. ''3-Dimensional ultrasound volume measurement,'' *Med. Phys.* **20,** 927 (1993).
39. M. Riccabona, T. R. Nelson, D. H. Pretorius, and T. E. Davidson. ''In-vivo three-dimensional sonographic measurement of organ volume: Validation in the urinary bladder,'' *J. Ultrasound Med.* **15,** 627–632 (1996).
40. T. R. Nelson, T. E. Davidson, and D. H. Pretorius. ''Interactive electronic scalpel for extraction of organs from 3DUS data,'' *Radiology* **197,** 191 (1995).
41. T. R. Nelson and D. H. Pretorius. ''Visualization of the fetal thoracic skeleton with 3-dimensional sonography: A preliminary report,'' *AJR* **164,** 1485–1488 (1995).
42. D. H. Pretorius and T. R. Nelson. ''Prenatal visualization of cranial sutures and fontanelles with 3-dimensional ultrasonography,'' *J. Ultrasound Med.* **13,** 871–876 (1994).